Published in final edited form as:
Vis Neurosci. 2005 ; 22(4): 493–500.

Spatiotemporal integration of light by the cat X-cell center under photopic and scotopic conditions

J.B. TROY[1], **D.L. BOHNSACK**[1], **J. CHEN**[1], **X. GUO**[1], and **C.L. PASSAGLIA**[1,2]
1*Department of Biomedical Engineering and the Neuroscience Institute, Northwestern University, Evanston*

2*Department of Biomedical Engineering, Boston University, Boston*

Abstract

Visual responses to stimulation at high temporal frequency are generally considered to result from signals that avoid light adaptive gain adjustment, simply reflecting linear summation of luminance. Under conditions of high photopic illuminance, the center of the receptive field of the cat X-cell has been shown to expand in size when stimulated at high temporal frequency, raising the possibility that there is spatiotemporal interaction in luminance summation. Here we show that this expansion maintains constant the product of the center's luminance summing area and the temporal period of luminance modulation, implying that spatial and temporal integration of luminance can be traded for one another by the X-cell center. As such the X-cell has a spatiotemporal window for luminance integration that fuses the classical concepts of a spatial window of luminance integration (Ricco's Law) with a temporal window of luminance integration (Bloch's Law). We were interested to determine whether this tradeoff between spatial and temporal summation of luminance occurs also at lower light levels, where the temporal-frequency bandwidth of the X-cell is narrower. We found that it does not. Center radius does not expand with temporal frequency under either low photopic or scotopic conditions. These results are discussed within the context of the known retinal circuitry that underlies the X-cell center for photopic and scotopic conditions.

Keywords

Contrast sensitivity; Retinal ganglion cell; Rod and cone inputs; Visual adaptation; Temporal frequency

Introduction

The optic nerves provide all visual input to the brain and the representation of visual information is most compact at this level of the visual system; there are fewer retinal ganglion cells to represent the visual world than there are neurons at any other stage. Retinal ganglion cells are also the first neurons in the visual system whose messages are encoded in trains of action potentials and, therefore, accessible to extracellular recording techniques. These two facts, allied with the key role of ganglion cells in the blinding disorder glaucoma, have made them a popular subject for study over the past fifty years (Troy & Shou, 2002). In spite of this degree of scrutiny, many properties of ganglion cell receptive fields remain incompletely characterized.

Address correspondence and reprint requests to: J.B. Troy, Department of Biomedical Engineering, McCormick School of Engineering & Applied Sciences, Northwestern University, 2145 Sheridan Road, Evanston, IL 60208-3107, USA. E-mail: j-troy@northwestern.edu.

Most retinal ganglion cells of higher mammals have center-surround receptive fields (Kuffler, 1953; Cleland & Levick, 1974*a*,*b*; Stone & Fukada, 1974; De Monasterio & Gouras, 1975). For such cell types, the size of the center region of the receptive field is known to play two crucial roles in the processing of visual information. Firstly, since luminance is integrated over the receptive-field center, its size sets the spatial-frequency bandwidth of the message sent to the brain by the ganglion cell (Enroth-Cugell & Robson, 1966; Linsenmeier et al., 1982), with smaller centers providing greater bandwidth. Secondly, the center region is known to correspond to the spatial pool for light adaptation (Enroth-Cugell & Shapley, 1973; Saito & Fukada, 1986; Cleland & Freeman, 1988), the process by which ganglion cells are made to signal luminance contrast (Troy & Enroth-Cugell, 1993), leading to an essentially invariant representation of objects irrespective of their illumination (Shapley & Enroth-Cugell, 1984).

Given its important function in information coding, it is surprising therefore that the size of the center of the cat X-cell—the most numerous ganglion cell of this species—is known to vary with temporal frequency. Under conditions of high photopic (cone-driven) vision, its center has been shown to expand at high temporal frequencies (Frishman et al., 1987; Troy & Enroth-Cugell, 1989). In this paper, we show that a simple relationship exists between center size and temporal frequency at high photopic light levels. The relationship that we find remains consistent with the notion that the center constitutes the pool for light adaptation, but indicates that, for these high photopic conditions, integration of light over space may be traded for integration over time in setting the adaptation pool. In contrast, we show that center size is invariant with temporal frequency under low photopic and under scotopic (rod-driven) conditions, implying that space and time integration of light are separable at these illuminances. We discuss how differences between the retinal circuits underlying photopic and scotopic vision might account for these different neural mechanisms of luminance integration and, presumably, light adaptation in the different ranges of illuminance.

Materials and methods

Animal preparation

Experiments were performed on adult cats. Anesthesia was induced with sodium pentothal (20 mg kg^{-1}, i.v.) or ketamine hydrochloride mixed with acepromazine (25 and 1 mg kg^{-1}, respectively, i.m) and maintained during preparatory surgery with supplemental doses of sodium pentothal. For the recording session, anesthesia was maintained with ethyl carbamate (15–50 mg kg^{-1} h^{-1} following a loading dose of 200 mg kg^{-1}, i.v.). The cats were paralyzed to minimize eye movements. Paralysis was achieved *via* a steady intraveneous infusion of pancuronium bromide (0.2 mg kg^{-1} h^{-1}) or gallamine triethiodide (10 mg kg^{-1} h^{-1}). Paralyzed animals were artificially ventilated and their blood pressure and heart rate monitored continuously to assess depth of anesthesia. Body temperature and end-tidal CO_2 were also measured and maintained at normal levels. Pupils were dilated with topical application of 1% atropine sulfate and nictitating membranes retracted with 10% phenylephrine hydrocholride. The eyes were fitted with artificial pupils (4–5 mm diameter) and the visual stimulus focused onto the retina with auxiliary lenses. Refraction was assessed by measuring the spatial-frequency resolution of central X-cells for lenses of different power; the lens that gave the cell's best resolution was chosen. All procedures were reviewed and approved by Northwestern University's Animal Care and Use Committee and are in accordance with NIH guidelines.

Visual stimulation and data collection

Full-screen-width sinusoidal luminance gratings and a bipartite field were the stimuli used for the work contained in this paper, with the bipartite field employed only for receptive-field alignment. Sinusoidal gratings were employed in two capacities: (1) for cell identification using the modified null test of Hochstein and Shapley (1976), and (2) to measure the spatial-

frequency filtering properties of X-cells across a range of temporal frequencies. Responsivity and the phase of the response were measured for each cell as a function of spatial frequency at a number of temporal frequencies. One was 2 Hz. The others were concentrated at high temporal frequencies (> 10 Hz for scotopic and low photopic conditions, > 30 Hz for high photopic conditions), since our objective was to determine how receptive-field center size depended on temporal frequency in this range. All measurements were based on responses with fundamental component amplitudes in the range of 5–10 impulses s^{-1}. This is a range in which X-cell responses scale linearly with contrast (Enroth-Cugell et al., 1983; Troy & Enroth-Cugell, 1993). Responsivity is defined as the amplitude of the fundamental component divided by the contrast that evoked the response. At least 30 s of discharge were used for each measurement, although longer records (> 1 min) were used typically for measurements taken for high temporal frequencies or scotopic conditions where the signal-to-noise ratio is low (Passaglia & Troy, 2004*a*,*b*). Two visual display units were used for different sets of measurements. One was a Joyce display running at 200 Hz with a luminance of 305–315 cd m^{-2}. The other was a Sony Trinitron display running at 150-Hz frame rate with a luminance of 30 cd m^{-2}. For some experiments, neutral density filters were placed in front of the visual display to bring its luminance, as seen by the cat, into the scotopic range. Retinal illuminance will be given as cat trolands (td), which in our usage is the product of photopic luminance (units of cd m^{-2})and pupil area (units of mm^2). One cat troland corresponds to a retinal illuminance of about 2–3 trolands. Illuminance in scotopic cat trolands is ~2.5 times higher than the photopic values given.

Receptive field model and data fitting

To obtain estimates of receptive-field center size and center responsivity, the X-cell receptive field was modeled as represented in eqn. (1):

$$\begin{aligned} \mathbf{R_c}(f, v) &= \mathbf{K_c}(f) \exp(-(\pi r_c(f) v)^2), \\ \mathbf{R_s}(f, v) &= \mathbf{K_s}(f) \exp(-(\pi r_s v)^2), \\ \mathbf{R}(f, v) &= \mathbf{R_c}(f, v) - \mathbf{R_c}(f, v) - \mathbf{R_s}(f, v). \end{aligned} \tag{1}$$

$\mathbf{R_c}$ and $\mathbf{R_s}$ are the spatiotemporal-frequency transfer functions of the center and surround of the receptive field, and $\mathbf{K_c}$ and $\mathbf{K_s}$ are their corresponding temporal-frequency transfer functions. $\mathbf{R}$ is the spatiotemporal-frequency transfer function of the cell. v is spatial frequency and f is temporal frequency. Both center and surround are assumed to have Gaussian spatial weighting with characteristic radii r_c and r_s (Rodieck, 1965; Enroth-Cugell & Robson, 1966), the former being a function of temporal frequency and the latter independent of temporal frequency (Frishman et al., 1987). The characteristic radius is the radial width of the center or surround mechanism when responsivity has declined by 1/e from its peak. K_c and K_s in eqn. (1) are complex quantities having both amplitude, $\mathbf{K_c}$ and $\mathbf{K_s}$, and phase, θ_c and θ_s. For the purposes of this paper, our interest is in K_c, r_c, and θ_c only and in their dependences on temporal frequency. Gauss®, a software package optimized by Aptech Systems Inc. (Maple Valley, WA) for IBM-compatible personal computers, was used for obtaining fits of eqn. (1) to the data. The root-mean-square error (r.m.s.) between the fit and the data was calculated in the complex plane and minimized by a nonlinear algorithm (BFGS: Dennis & Schnabel, 1983). Some fits were also made in MatLab with similar results. The fits provided the estimates of K_c and r_c that were used in the Results section.

Results

Dependence of center radius on temporal frequency under high photopic illuminance

From a number of studies, we know that the radius of the center of the X-cell receptive field is invariant with temporal frequency in the range 0.5 to 30 Hz at high photopic illuminance (Enroth-Cugell et al., 1983; Dawis et al., 1984; Troy & Enroth-Cugell; 1993). At higher temporal frequencies, however, the X-cell center expands (Frishman et al., 1987; Troy & Enroth-Cugell; 1993). On double-logarithmic coordinates Fig. 1A plots data from the most extensive study of this phenomenon (Troy & Enroth-Cugell, 1989), showing how the size of the X-cell receptive-field center, normalized to its value at 2 Hz (see legend to Fig. 1A), varies as a function of temporal frequency. A least-squares regression line with a slope of 0.52 (the line of thick dots in Fig. 1A) fits the 50–70 Hz data very well (correlation coefficient, 0.984). Since the slope of the regression line is close to 0.5, a very good empirical model for the dependence of center size upon temporal frequency under photopic conditions is given by the expression:

$$r_c(f) = \begin{cases} r_{c,2\text{Hz}}\sqrt{\frac{f}{f_c}}, & \text{for } f \geq f_c, \\ r_{c,2\text{Hz}}, & \text{for } f < f_c, \end{cases} \quad (2)$$

where $r_{c,2\text{Hz}}$ is center radius at 2 Hz, f is temporal frequency, and f_c is the temporal frequency above which center size expands. In the case of the data shown in Fig. 1A, f_c is 42 Hz. The solid line in Fig. 1A is eqn. (2). An interesting way of stating this result is that center radius expands just enough to permit the product of center area and temporal period (the reciprocal of temporal frequency) to maintain a constant value. Hence, in the sense that the area of the center mechanism has long been considered to act as a spatial window for luminance integration by an X-cell, the product of the center's area and the temporal period can be considered a spatiotemporal window of luminance integration.

How f_c relates to the temporal-frequency filtering properties of X-cells is of interest. From Frishman et al. (1987), we know that under the level of photopic lighting at which the data of Fig. 1A were collected, the responsivity of the center mechanism of the X-cell receptive field remains more or less constant from 1 Hz to ~30 Hz. For temporal frequencies beyond 40 Hz, responsivity declines steeply and monotonically with increasing frequency, often preceded by a small peak is responsivity. The data points in Fig. 1B plot the average X-cell center responsivities (K_c) at 2, 40, 50, 60, and 70 Hz for the X-cells used to generate Fig. 1A. The 50–70 Hz points of Fig. 1B are well fit by a regression line that intersects the line of constant responsivity drawn through the 2-Hz point at a temporal frequency of 40 Hz. This is very close, and within experimental uncertainty, to the 42-Hz frequency at which we estimate that center expansion starts. One can conclude therefore that the expansion in center size begins more or less at the temporal frequency where the responsivity of the center mechanism transitions from a plateau of constant responsivity to its high frequency roll-off; that is, the corner frequency.

Interestingly, the corner frequency also demarcates the frequency band of light-adapted visual signals. Many investigators have pointed out that visual sensitivity to luminance flicker is independent of mean light level for frequencies above but not below the corner frequency (e.g. Kelly, 1972; Tranchina et al., 1984; Graham & Hood, 1992). Thus, the expansion in center radius occurs over the range of frequencies where visual signals are free from the influence of light adaptation, meaning the range within which visual signals result from simple linear summation of luminance. Fig. 2 shows in the form of a block diagram a model that accounts for the frequency-dependent transition from linear (nonadapted) to nonlinear (adapted) visual signaling.

Fig. 2A shows that the visual output is a time-varying signal $r(t)$ that results from the operation of $h(x, y, t)$ on the time-varying input luminance signal $L(x, y, t)$. The operation $h(x, y, t)$ is nonlinear and incorporates light adaptation. Fig. 2B is an unpacking of $h(x, y, t)$. The through path represents an initial linear operation where $h_1(x, y, t)$ summates the input luminance signal $L(x, y, t)$ over space and time, giving rise to the signal $r(t)$. Mathematically, we can represent the operation as

$$r(t) = \iiint h_1(\xi, \psi, \tau) L(x - \xi, y - \psi, t - \tau) \, d\xi \, d\psi \, d\tau. \quad (3)$$

Were space and time to be separable, $h_1(\xi, \psi, \tau)$ in eqn. (3) could be replaced by

$$h_1(\xi, \psi, \tau) = h_{1,S}(\xi, \psi) h_{1,t}(\tau), \quad (4)$$

and integration over space and time performed separately. This would be the case were center size not to depend on frequency. In such a case, $h_{1,S}(\xi, \psi)$ would be the luminance spatial weighting function of the X-cell center, generally modeled as a Gaussian function (Rodieck, 1965; Enroth-Cugell & Robson, 1966), and $h_{1,t}(\tau)$ would be the X-cell center's impulse response. However, the results of Fig. 1 imply that eqn. (4) is invalid in this case and $h_1(\xi, \psi, \tau)$ cannot be separated into space and time functions.

The feedback loop of Fig. 2B represents the pathway for light adaptation, along the lines of models proposed by Fuortes and Hodgkin (1964),Tranchina et al. (1984), and Victor (1987). Consider $r(t)$ to be initially a nonadapted visual signal generated in response to a spatiotemporal change in luminance. Light adaptation modifies $h_1(t)$ and thus $r(t)$ by adaptive gain control. The degree of gain adjustment is controlled by feedback and the signal that adjusts gain, $g(t)$, is a low-pass filtered (time-integrated) version of the output signal $r(t)$. As drawn, it is

$$g(t) = \int h_2(\tau) r(t - \tau) \, d\tau. \quad (5)$$

The diamond ending symbolizes a nonlinear operation. In Fuortes and Hodgkin's (1964) model of adaptation in the *Limulus* eye, feedback decreases membrane resistance leading to a reduction in signal gain and duration of the impulse response, $h_1(t)$. The result is attenuation of low frequencies and an increase in the frequency bandwidth of $h_1(t)$. As light level increases the corner frequency that demarcates linear (without adaptation) from nonlinear (adapted) visual signals moves to progressively higher frequencies (Fuortes & Hodgkin, 1964; Pinter, 1966). If a similar model applies to the X-cell center, one would predict that the corner frequency of its responsivity *versus* temporal-frequency function should rise with light level. This is borne out by experimental results (Frishman et al., 1987).

Given that the data presented in Fig.1 show that, for high temporal frequencies, there is a tradeoff between temporal integration by the X-cell center and the spatial field of luminance summation for photopic nonadapted visual signals, it is of interest whether this tradeoff between integration of luminance over space and time applies at other light levels too. This is important both as a step towards understanding retinal mechanisms of light adaptation and in that it bears upon two venerable psychophysical laws. Bloch's Law states that the visual response to a flash of light is the same for flashes that deliver the same number of quanta within a critical time window t_c no matter how those quanta are distributed temporally over that window, which we will refer to as the visual integration time. Ricco's Law states that the visual response to a flash of light is the same for flashes that deliver the same number of quanta within a critical spatial window A_s no matter how those quanta are distributed spatially over that window. One can consider A_s to be the summation area for integration of luminance. Since the visual integration time is inversely proportional to the corner frequency (Roufs, 1972*a*,*b*) and

the X-cell center is a critical area of luminance summation for visual signals in the cat, eqn. (2) implies that Bloch's and Ricco's Laws would be nonseparable in the range of high photopic illuminance. That Roufs (1972*a*,*b*) showed inverse proportionality to hold across a range of mean light levels, one wonders whether t_c and A_s might trade-off with one another at all mean light levels.

No dependence of center radius on temporal frequency under scotopic illuminance

Fig. 3A shows plots of responsivity *versus* spatial frequency for an ON-center X-cell measured for a set of three temporal frequencies at a light level for which the cell is driven by signals originating with rod photoreceptors. The retinal illuminance is ~0 log cat td, a light level about 30-fold lower than the one at which cat X-cell responses transition from the rod-driven to the cone-driven state (Chan et al., 1992;Troy et al., 1999). From these curves, specifically the dependence of responsivity upon spatial frequency for optimal to high spatial frequencies, we were able to obtain accurate estimates of receptive-field center radius. Fig. 3B plots the ratio $r_c/r_{c,2\ \mathrm{Hz}}$ for this cell across the three temporal frequencies shown in Fig. 3A and two others. There was essentially no change. This experiment was repeated with 14 other cells, and Fig. 3C shows the relationship between $r_c/r_{c,2\ \mathrm{Hz}}$ and f for the average across all cells (13 ON-center and 2 OFF-center cells). Error bars are standard errors. In contrast to the results obtained for high photopic conditions, it is clear that center radius is invariant with temporal frequency in the scotopic range.

No dependence of center radius on temporal frequency under low photopic illuminance

The fact that the size of the receptive-field center of the X-cell was invariant with temporal frequency under scotopic conditions led us to question whether or not center size expands with temporal frequency at all photopic light levels. Since the retinal circuitry for scotopic and photopic vision is very different (Smith et al., 1986), it seemed quite possible that the expansion of center size at high temporal frequencies might be a universal property of photopic signals. To investigate this question, we examined the effect of temporal frequency on center radius at a low photopic light level. For 26 X-cells (16 ON-center and 10 OFF-center cells), spatial-frequency responses were measured at a set of temporal frequencies at a retinal illuminance of 2.5 log cat td, which is in the low photopic range. Rod saturation occurs at 1–2 log cat td (Lennie et al., 1976). Fits of eqn. (1) to the spatial-frequency responses were comparable to the data shown in Fig. 3A. Fig. 4A plots, for the average of these 26 X-cells, the center radius normalized to the radius at 2 Hz as a function of temporal frequency, like in Fig. 1A. Little data were collected at 10 Hz, once we had determined that this frequency was below the corner frequency of the responsivity *versus* temporal-frequency relationship (Fig. 4B), explaining the large error bars for this data point of Fig. 4A. The corner frequency is at ~16 Hz and the dotted line in Fig. 4A plots eqn. (2) with f_c as 16 Hz. Clearly, the data give no indication that center radius depends on temporal frequency at this light level either. Hence, center radius is invariant with temporal frequency at low photopic as well as at scotopic light levels.

The temporal-frequency dependence of center size

Combining the photopic data (Fig. 5A), one finds that the dependence of center size upon temporal frequency can be reconciled into one relationship given by eqn. (6):

$$r_c(f) = \begin{cases} r_{c,2\mathrm{Hz}}\sqrt{\dfrac{f}{f_c}}, & \text{for } f \geq 40\ Hz, \\ r_{c,2\mathrm{Hz}} & \text{for } f < 40\ \mathrm{Hz}. \end{cases} \tag{6}$$

In fact, the scotopic data are also consistent with this relationship (Fig. 5B), since the scotopic temporal-frequency response of X-cells does not extend to 40 Hz. Thus, it seems that eqn. (6)

provides a full characterization of the dependence of the X-cell center size on temporal frequency across all light levels.

Discussion

The key results are as follows:

1. At high photopic illuminance, the receptive-field center of an X-cell expands at high temporal frequency, expanding just enough to keep the product of center area and temporal period constant;
2. Under scotopic and low photopic conditions, the center size of the X-cell is invariant with temporal frequency.

Functional significance

The visual threshold ($\mathcal{C}_t$) for detection of flashes of light of luminance L and duration Δt can be expressed mathematically as

$$\mathcal{C}_t = L \cdot \Delta t \text{ for } \Delta t \leq t_c, \tag{7}$$

where $\mathcal{C}_t$ is a constant. This relationship is known as Bloch's Law and says that luminance can be traded for time as long as Δt is less than the *integration time* t_c. Similarly, the visual threshold ($\mathcal{C}_A$) for detection of flashes of light of luminance L and area A can be expressed mathematically as

$$\mathcal{C}_A = L \cdot A \text{ for } A \leq A_s, \tag{8}$$

where $\mathcal{C}_A$ is a constant. This relationship is known as Ricco's Law and says that luminance can be traded for stimulus area as long as A is less than the *summation area* A_s. To the extent that the X-cell center provides a physiological substrate for threshold integration of luminance, our results suggest that under high photopic, but not low photopic or scotopic, conditions A_s and t_c can be traded for one another as long as the product $A_s \cdot t_c$ is held constant. We believe therefore that Bloch's and Ricco's Laws should be combined for high photopic conditions to give the relationship:

$$\mathcal{C} = L \cdot A \cdot \Delta t, \quad \text{for } \Delta t \leq t_c \text{ and } A \cdot \Delta t \leq A_S \cdot t_c, \tag{9}$$

where $\mathcal{C}$ is a constant. Under low photopic and scotopic conditions, our data indicate that a similar consolidation of Bloch's and Ricco's Laws is not possible.

Retinal circuitry

Given that the X-cell center expands under high photopic but not under low photopic or scotopic conditions, a reasonable initial hypothesis is that the expansion reflects lateral signal flow within the network of cones. Light-evoked signals generated in cat cones can spread laterally across the retina through the electrical junctions that couple cones together (Kolb, 1977; Smith et al., 1986). For these signals to spread further at high than low temporal frequencies, it is well known that the cones would need to have appropriate voltage-sensitive conductance mechanisms that are activated with a comparatively slow time-course so that current spread through the network is short-circuited at low but not high temporal frequencies (Detwiler et al., 1978, 1980; Attwell et al., 1984; Koch, 1984). Studies of the inner segment properties of all vertebrate photoreceptors examined to date suggest that such conductance mechanisms would be present in cat cones (e.g. Brown & Pinto, 1974; Bader et al., 1979, 1982; Attwell et

al., 1982; Corey et al., 1984; Hestrin, 1987; Maricq & Korenbrot, 1988, 1990; Barnes & Hille, 1989; Yagi & MacLeish, 1994; Schneeweis & Schnapf, 1995; Demontis et al., 1999), so the necessary anatomical and biophysical substrates for the center expansion are present (Fig. 6).

We consider the inner segment I_h conductance to be one plausible candidate (some of the other inner segment voltage-sensitive conductances could work as well). I_h is a significant cationic conductance that is activated by a threshold membrane hyperpolarization (Hestrin, 1987; Demontis et al., 1999), the hyperpolarization needed to reach threshold decreasing obviously as the cone's resting potential hyperpolarizes with ambient light level. Now, the time-course of activation of the I_h conductance is known to accelerate with hyperpolarization (Hestrin, 1987), so in addition to providing a biophysical substrate for an increase in center radius with temporal frequency, the I_h conductance together with cone coupling would create an interesting spatiotemporal interaction. One would predict that, if I_h underlies the center expansion shown in Fig. 1A, the corner for expansion would occur at progressively higher frequencies with increasing light level. This could permit the corner for X-cell center expansion to increase in lockstep with the corner frequency, which is well known to increase with light level (Roufs, 1972*a*,*b*). In other words, this mechanism might permit the X-cell center to maintain a constant size over the full temporal-frequency range of peak responsivity, even as this range broadens at higher light levels than the highest shown here. However, because of pupillary constriction, the cat retina is never illuminated naturally with much more than our high photopic light level (Hammond & Mouat, 1985; Oh et al., 1995) so any such effect would be minor. Consequently, the data presented in Fig. 5B and the relationship given by eqn. (6) are essentially complete for the X-cell.

One might wonder why, if this explanation were correct, rod signals in cones (Nelson, 1977) should not be subject to the same mechanism. They would be. However, rod saturation occurs at 1–2 log cat td (Lennie et al., 1976) so the effect of rod input at this and higher light levels should be just a steady hyperpolarization of the cone membrane potential. Rod signals at the photopic light levels investigated here are therefore unmodulated.

Summary

The preceding discussion emphasized what mechanism might explain the change in X-cell center radius with temporal frequency that occurs at high light levels. It is important, however, that one should not lose sight of the key observation that the X-cell center size is maintained constant over its primary operational range. A major function of the I_h and some other conductances in the cone's inner segment is presumably to increase signal bandwidth at light levels when signal-to-noise is good. It is likely that center expansion occurs because these conductances are not activated at high temporal frequencies. It is signals at the lower temporal frequencies in the X-cell spike train that are of functional relevance as Passaglia and Troy (2004*a*,*b*) have argued recently. Activation of the I_h and other voltage-sensitive conductances also reduce signal amplitude at low frequencies, contributing to light adaptation.

Acknowledgements

Drs. Ch. Enroth-Cugell and M. Vorobyev are thanked for their comments on drafts of the manuscript. The work was supported by NIH R01 EY06669.

References

Attwell D, Werblin FS, Wilson M. The properties of single cones isolated from the tiger salamander retina. Journal of Physiology 1982;328:259–283. [PubMed: 7131315]

Attwell D, Wilson M, Wu SM. A quantitative analysis of interactions between photoreceptors in the salamander (*Ambystoma*) retina. Journal of Physiology 1984;352:703–737. [PubMed: 6747904]

Bader CR, Bertrand D, Schwartz EA. Voltage-activated and calcium-activated currents studied in solitary rod inner segments from the salamander retina. Journal of Physiology 1982;331:253–284. [PubMed: 7153904]

Bader CR, MacLeish PR, Schwartz EA. A voltage-clamp study of the light response in solitary rods of the tiger salamander. Journal of Physiology 1979;296:1–26. [PubMed: 529060]

Barnes S, Hille B. Ionic channels of the inner segment of tiger salamander cone photoreceptors. Journal of General Physiology 1989;94:719–743. [PubMed: 2482325]

Brown JE, Pinto LH. Ionic mechanism for the photoreceptor potential of the retina of *Bufo Marinus.* Journal of Physiology 1974;236:575–591. [PubMed: 4207130]

Chan LH, Freeman AW, Cleland BG. The rod-cone shift and its effect on ganglion cells in the cat retina. Vision Research 1992;32:2209–2219. [PubMed: 1287998]

Cleland BG, Freeman AW. Visual adaptation is highly localized in the cat's retina. Journal of Physiology 1988;404:591–611. [PubMed: 3253443]

Cleland BG, Harding TH, Tulunay-Keesey U. Visual resolution and receptive-field size: Examination of two kinds of cat retinal ganglion cell. Science 1979;205:1015–1017. [PubMed: 472720]

Cleland BG, Levick WR. Brisk and sluggish concentrically organized ganglion cells in the cat's retina. Journal of Physiology 1974a;240:421–456. [PubMed: 4421622]

Cleland BG, Levick WR. Properties of rarely encountered types of ganglion cells in the cat's retina and an overall classification. Journal of Physiology 1974b;240:457–492. [PubMed: 4420300]

Corey DP, Dubinsky JM, Schwartz EA. The calcium current in inner segments of rods from the salamander (*Ambystoma tigrinum*) retina. Journal of Physiology 1984;354:557–575. [PubMed: 6090654]

Dawis S, Shapley R, Kaplan E, Tranchina D. The receptive field organization of X-cells in the cat: Spatiotemporal coupling and asymmetry. Vision Research 1984;24:549–564. [PubMed: 6740975]

De Monasterio FM, Gouras P. Functional properties of ganglion cells of the rhesus monkey retina. Journal of Physiology 1975;251:167–195. [PubMed: 810576]

Demontis GC, Longoni B, Barcaro U, Cervetto L. Properties and functional roles of hyperpolarization-gated currents in guinea-pig retinal rods. Journal of Physiology 1999;515.3:813–828. [PubMed: 10066907]

Dennis, J.E. Jr & Schnabel, R.B. (1983). *Numerical Methods for Unconstrained Optimization and Nonlinear Equations* Englewood Cliffs, New Jersey: Prentice Hall.

Detwiler PB, Hodgkin AL, McNaughton PA. A surprising property of electrical spread in the network of rods in the turtle's retina. Nature 1978;274:562–565. [PubMed: 672987]

Detwiler PB, Hodgkin AL, McNaughton PA. Temporal and spatial characteristics of the voltage response of rods in the retina of the snapping turtle. Journal of Physiology 1980;300:213–250. [PubMed: 7381784]

Enroth-Cugell C, Robson JG. The contrast sensitivity of retinal ganglion cells of the cat. Journal of Physiology 1966;187:517–552. [PubMed: 16783910]

Enroth-Cugell C, Shapley RM. Flux, not retinal illumination, is what cat retinal ganglion cells really care about. Journal of Physiology 1973;233:311–326. [PubMed: 4747230]

Enroth-Cugell C, Robson JG, Schweitzer-Tong DE, Watson AB. Spatiotemporal interactions in cat retinal ganglion cells showing linear spatial summation. Journal of Physiology 1983;341:279–307. [PubMed: 6620181]

Frishman LJ, Freeman AW, Troy JB, Schweitzer-Tong D, Enroth-Cugell C. Spatiotemporal frequency responses of cat retinal ganglion cells. Journal of General Physiology 1987;89:599–628. [PubMed: 3585279]

Fuortes MGF, Hodgkin AL. Changes in time scale and sensitivity in the ommatidia of *Limulus.* Journal of Physiology 1964;156:179–192. [PubMed: 13702633]

Graham N, Hood DC. Modeling the dynamics of light adaptation: The merging of two traditions. Vision Research 1992;32:1373–1393. [PubMed: 1455710]

Hammond P, Mouat GSV. The relationship between feline pupil size and luminance. Experimental Brain Research 1985;59:485–490.

Hestrin S. The properties and function of inward rectification in rod photoreceptors of the tiger salamander. Journal of Physiology 1987;390:319–333. [PubMed: 2450992]

Hochstein S, Shapley RM. Quantitative analysis of retinal ganglion cell classifications. Journal of Physiology 1976;262:237–264. [PubMed: 994039]

Kelly DH. Adaptation effects on spatio-temporal sine-wave thresholds. Vision Research 1972;12:89–101. [PubMed: 5034636]

Koch C. Cable theory in neurons with active, linearized membranes. Biological Cybernetics 1984;50:15–33. [PubMed: 6324889]

Kolb H. The organization of the outer plexiform layer in the retina of the cat: Electron microscopic observations. Journal of Neurocytology 1977;6:131–153. [PubMed: 856949]

Kuffler SW. Discharge patterns and functional organization of mammalian retina. Journal of Neurophysiology 1953;16:37–68. [PubMed: 13035466]

Lennie P, Hertz BG, Enroth-Cugell C. Saturation of rod pools in cat. Vision Research 1976;16:935–940. [PubMed: 948882]

Linsenmeier RA, Frishman LJ, Jakiela HG, Enroth-Cugell C. Receptive field properties of X and Y cells in the cat retina derived from contrast sensitivity measurements. Vision Research 1982;22:1173–1183. [PubMed: 7147728]

Maricq AV, Korenbrot JI. Calcium and calcium-dependent chloride currents generate action potentials in solitary cone photoreceptors. Neuron 1988;1:503–515. [PubMed: 2483100]

Maricq AV, Korenbrot JI. Inward rectification in the inner segment of single retinal cone photoreceptors. Journal of Neurophysiology 1990;64:1917–1928. [PubMed: 1705964]

Oh JK, Bohnsack DL, Troy JB, Enroth-Cugell Ch. The cat's pupillary light response under urethane anesthesia. Visual Neuroscience 1995;12:281–284. [PubMed: 7786849]

Passaglia CL, Troy JB. Information transmission rates of cat retinal ganglion cells. Journal of Neurophysiology 2004a;91:1217–1229. [PubMed: 14602836]

Passaglia CL, Troy JB. The impact of noise on retinal coding of visual signals. Journal of Neurophysiology 2004b;92:1023–1033. [PubMed: 15071086]

Peichl L, Wässle H. Size, scatter, and coverage of ganglion cell receptive field centers in the cat retina. Journal of Physiology 1979;291:117–141. [PubMed: 480198]

Pinter RB. Sinusoidal and delta function responses of visual cells of the *Limulus* eye. Journal of General Physiology 1966;49:565–593. [PubMed: 5938828]

Rodieck RW. Quantitative analysis of cat retinal ganglion cell response to visual stimuli. Vision Research 1965;5:583–601. [PubMed: 5862581]

Roufs JAJ. Dynamic properties of vision—I. Experimental relationships between flicker and flash thresholds. Vision Research 1972a;12:261–278. [PubMed: 5033689]

Roufs JAJ. Dynamic properties of vision—II. Theoretical relationships between flicker and flash thresholds. Vision Research 1972b;12:279–292. [PubMed: 5033690]

Saito H, Fukada Y. Gain control mechanisms in X- and Y-type retinal ganglion cells of the cat. Vision Research 1986;26:391–408. [PubMed: 3727406]

Schneeweis DM, Schnapf JL. Photovoltage of rods and cones in the macaque retina. Science 1995;268:1053–1056. [PubMed: 7754386]

Shapley R, Enroth-Cugell C. Visual adaptation and retinal gain controls. Progress in Retinal Research 1984;3:263–343.

Smith RG, Freed MA, Sterling P. Microcircuitry of the dark-adapted cat retina: Functional architecture of the rod–cone network. Journal of Neuroscience 1986;6:3505–3517. [PubMed: 3794785]

Stone J, Fukada Y. Properties of cat retinal ganglion cells: A comparison of W-cells with X- and Y-cells. Journal of Neurophysiology 1974;37:722–748. [PubMed: 4600539]

Tranchina D, Gordon J, Shapley RM. Retinal light adaptation—evidence for a feedback mechanism. Nature 1984;310:314–316. [PubMed: 6462216]

Troy JB, Enroth-Cugell C. The dependence of center radius on temporal frequency for the receptive fields of X retinal ganglion cells of cat. Journal of General Physiology 1989;94:987–995. [PubMed: 2614373]

Troy JB, Robson JG. Steady discharges of X and Y retinal ganglion cells of cat under photopic illuminance. Visual Neuroscience 1992;9:535–553. [PubMed: 1450106]

Troy JB, Enroth-Cugell C. X and Y ganglion cells inform the cat's brain about contrast in the retinal image. Experimental Brain Research 1993;93:383–390.

Troy JB, Shou T. The receptive fields of cat retinal ganglion cells in physiological and pathological states: Where we are after half a century of research. Progress in Retinal and Eye Research 2002;21:263–302. [PubMed: 12052385]

Troy JB, Bohnsack DL, Diller LC. Spatial properties of the cat X-cell receptive field as a function of mean light level. Visual Neuroscience 1999;16:1089–1104. [PubMed: 10614589]

Victor JD. The dynamics of the cat retinal X cell centre. Journal of Physiology 1987;386:219–246. [PubMed: 3681707]

Yagi T, MacLeish PR. Ionic conductances of monkey solitary cone inner segments. Journal of Neurophysiology 1994;71:656–665. [PubMed: 7513752]

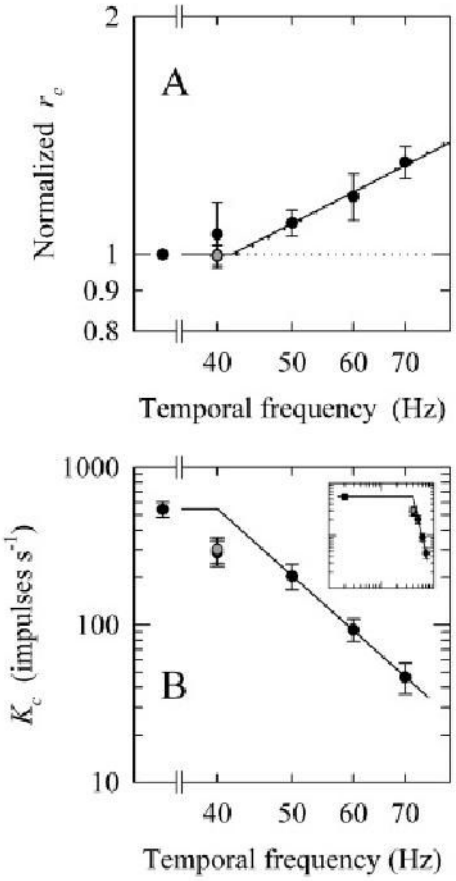

Fig. 1.

Frequency-dependent expansion of photopic center. (A) Plot of normalized center radius *versus* temporal frequency for X-cells under photopic illuminance. The normalization was performed because center size varies with retinal eccentricity (e.g. Cleland et al., 1979; Peichl & Wässle, 1979). Normalization involved dividing center radius for a particular cell and temporal frequency by its value at 2 Hz. This permitted us to quantify the fractional expansion in center size for each cell before averaging across cells. The data come from 16 X-cells (12 ON-center and 4 OFF-center cells). A complete set of data was not collected for all cells for all temporal frequencies. Each data point represents, therefore, the average of all cells for which an estimate of normalized center size could be obtained for that temporal frequency. Data from the following numbers of cells were averaged for each frequency: 16 at 2 Hz, 13 at 40 Hz, 12 at 50 Hz, 11 at 60 Hz, and 9 at 70 Hz. The 2-Hz point is plotted to the left of the broken abscissa. The line of thick dots running through the 50–70 Hz points is the best-fitting least-squares regression line. The solid line running through all points is eqn. (1). For all points, the error bars are standard errors. Only the 50-, 60-, and 70-Hz error bars show no overlap with the line of thin dots that indicates constant radius; that is, $r_c = r_{c,2\ \mathrm{Hz}}$. One outlier caused the 40-Hz point to lie above the $r_c = r_{c,2\ \mathrm{Hz}}$ line. With this outlier removed the 40-Hz point (grey circle) lies along this line and shows much less variance. (B) Plot on double-logarithmic coordinates of average center responsivity *versus* temporal frequency for the X-cells of panel (A). Error bars are standard errors. The corner frequency is 40 Hz. The inset shows the same data as a standard Bode plot (i.e. without the temporal-frequency axis expanded).

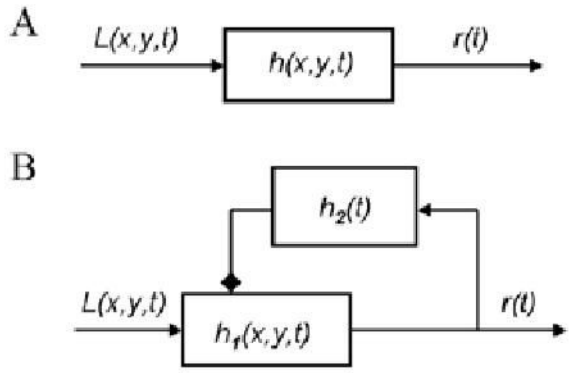

Fig. 2.

Feedback model of light adaptation. (A) A block diagram showing the transformation from a space- and time-varying pattern of luminance, $L(x, y, t)$, to a time-varying signal, $r(t)$. Under the assumption that the X-cell center constitutes the spatial pool for light adaptation (Enroth-Cugell & Shapley, 1973; Saito & Fukada, 1986; Cleland & Freeman, 1988), $h(x, y, t)$ is the signal processing operation performed on the visual input by an X-cell receptive-field center and incorporates both linear (luminance summation) and nonlinear (light adaptation) elements. (B) An unpacking of $h(x, y, t)$. The through path represents an initial linear operation where $h_1(x, y, t)$ summates the input luminance signal $L(x, y, t)$ over space and time, giving rise to the signal $r(t)$. The feedback loop represents the pathway for light adaptation, along the lines of models proposed by Fuortes and Hodgkin (1964), Tranchina et al. (1984) and Victor (1987). $r(t)$ is low-pass filtered and modifies $h_1(x, y, t)$, reducing the gain and increasing the temporal-frequency bandwidth of this filter. The diamond ending to the feedback path indicates a nonlinear (adaptive) operation.

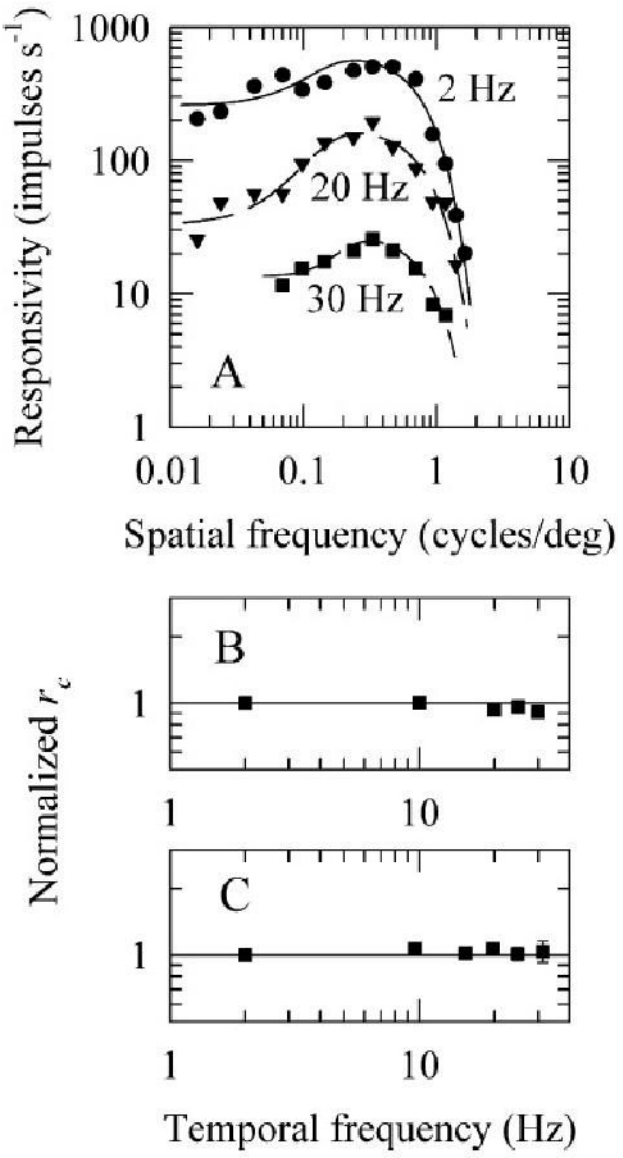

Fig. 3.

Scotopic center size is independent of temporal frequency. (A) Responsivity *versus* spatial-frequency curves at three temporal frequencies for an ON-center X-cell at scotopic illuminance (~0 log cat td). (B) Normalized center radius as a function of temporal frequency for the ON-center X-cell of panel A. (C) Normalized center radius as a function of temporal frequency for X-cells under scotopic conditions. The data points are the average of 13 ON-center and 2 OFF-center X-cells. It was not possible to collect data for all frequencies on all cells. The number of cells for each frequency were 15 at 2 Hz, 6 at 7.5 Hz, 15 at 11 Hz, 15 at 15 Hz, 15 at 19 Hz, 15 at 24 Hz, and 9 at 30 Hz. The error bars for the 30-Hz points are standard errors. For all other points standard errors are no larger than the points themselves.

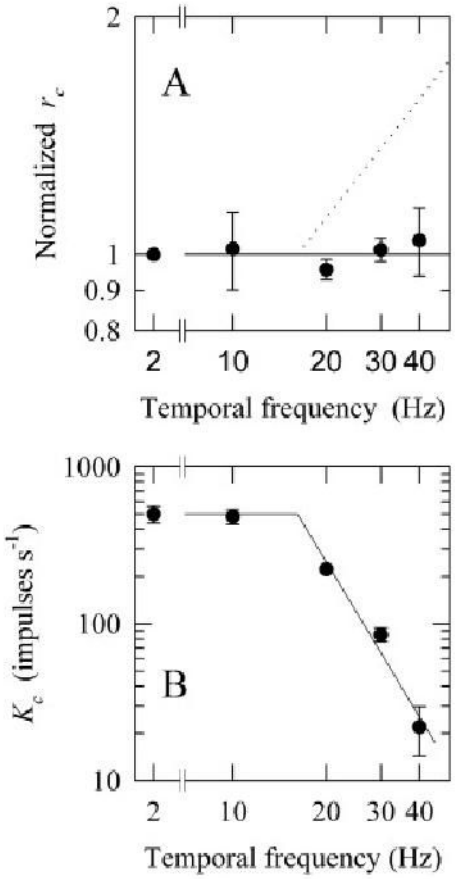

Fig. 4.

X-cell center size is independent of temporal frequency at low photopic light levels. (A) Plot of normalized center radius *versus* temporal frequency for X-cells under low photopic illuminance. The data points are the average of 26 X-cells (16 ON-center and 10 OFF-center cells). Each data point represents, therefore, the average of all cells for which an estimate of normalized center size could be obtained for that temporal frequency. Data from the following numbers of cells were averaged for each frequency: 26 at 2 Hz, 2 at 10 Hz, 22 at 20 Hz, 23 at 30 Hz, and 12 at 40 Hz. The 2-Hz point is plotted to the left of the broken abscissa. The line of dots is eqn. (1) with f_c = 16 Hz. Error bars are standard errors. (B) Plot on double-logarithmic coordinates of the average center responsivity *versus* temporal frequency for the X-cells of panel (A). Error bars are standard errors. The corner frequency is 16 Hz.

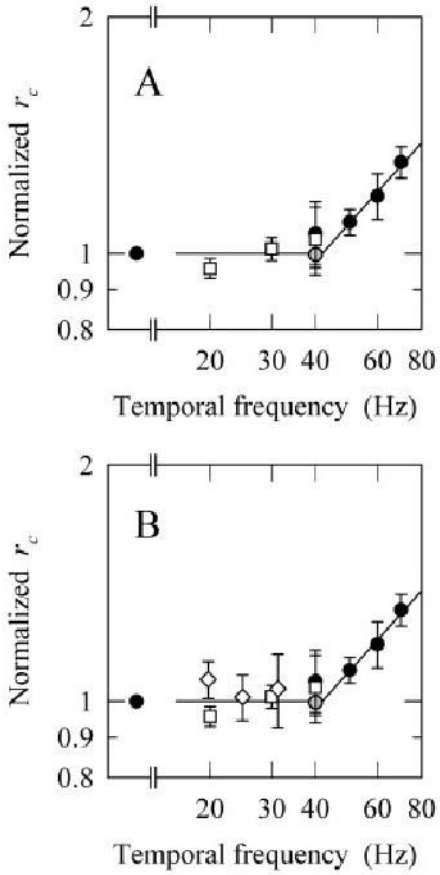

Fig. 5.

Dependence of X-cell center size on temporal frequency. (A) Normalized X-cell photopic center radius as a function of temporal frequency. Circles are data for high photopic light levels. Squares are data for low photopic light levels. The solid line is eqn. (1). (B) Normalized X-cell center radius as a function of temporal frequency. As for panel (A) with the scotopic data (diamonds) added.

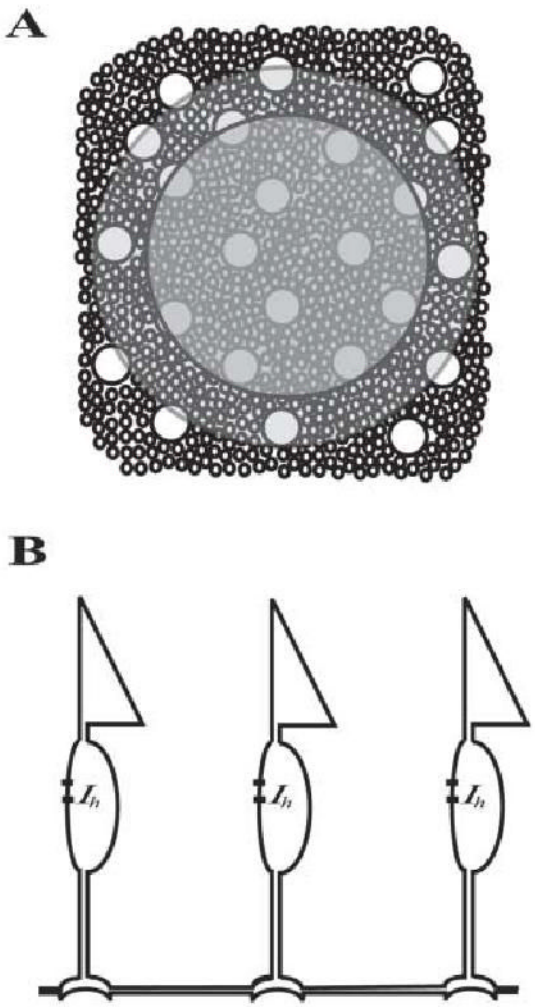

Fig. 6.

Possible model of X-cell center expansion. (A) Schematic drawing of the relationship between a rod and cone mosaic and the X-cell center. The cones are the large circles and the rods the small ones. The receptive-field center of the X-cell is assumed to encompass ~10 cones at low temporal frequencies (inner shaded large circle). At higher temporal frequencies, the X-cell center expands. Here an example is shown where the center has expanded to contain ~16 cones (outer shaded large circle), representing the kind of expansion seen at 70 Hz in Fig. 1. (B) Cones are coupled to each other in the cat retina through gap junctions. The inner segments of cones contain voltage-sensitive conductances, one of which produces the current I_h. This cationic conductance is activated by hyperpolarization, has a threshold and time of activation that shortens with membrane hyperpolarization below this threshold. The electrical coupling of cones together with the I_h conductance provides a plausible biophysical model for X-cell center expansion with temporal frequency at high photopic light levels. This model is also consistent with no expansion at low photopic light levels where the resting membrane potential of cones presumably sits well above the I_h threshold and no expansion under scotopic conditions where X-cells have a narrow temporal bandwidth.